

# Renormalizing into the mesoscopic quantum Hall insulator

PHILIPP CAIN<sup>1</sup> AND RUDOLF A. RÖMER<sup>2</sup>

<sup>1</sup> *Institut für Physik, Technische Universität Chemnitz, 09107 Chemnitz, Germany*

<sup>2</sup> *Department of Physics, University of Warwick, Coventry CV4 7AL, UK*

PACS. 73.43.-f – Quantum Hall effects.

PACS. 73.43.Nq – Quantum phase transitions.

PACS. 64.60.Ak – Renormalization-group, fractal, and percolation studies of phase transitions (see also 61.43.Hv Fractals; macroscopic aggregates).

**Abstract.** – Using the Chalker-Coddington network model as a drastically simplified, but universal model of integer quantum Hall physics, we investigate the plateau-to-insulator transition at strong magnetic field by means of a real-space renormalization approach. Our results suggest that for a fully quantum coherent situation, both the Hall insulator with diverging Hall resistance  $R_H$  and the quantized Hall insulator with  $R_H \approx h/e^2$  can be observed depending on the precise nature of the averaging procedure.

*Introduction.* – The integer quantum Hall (QH) transitions are described well in terms of a series of delocalization-localization transitions of the electron wavefunction [1, 2, 3, 4, 5, 6, 7, 8, 9, 10, 11]. These universal plateau-plateau transitions are accompanied by a power-law divergence  $\epsilon^{-\nu}$  of the electronic localization length  $\xi$ , where  $\epsilon$  defines the distance to the transition for a suitable controlled parameter, e.g. the electron energy [8, 9, 10]. Similarly, it is now conclusively established that plateau-plateau and insulator-plateau transitions exhibit the same critical behavior [12, 13, 14, 15, 16, 17, 18, 19, 20, 11, 21].

However, the value of the Hall resistivity  $R_H$  in this insulating phase (at large magnetic field) is still rather controversial. Various experiments have found that  $R_H$  remains very close to its quantized value  $h/e^2$  even deep in the insulating regime [12, 13, 14, 16, 17, 18, 21] with longitudinal resistance  $R_L > h/e^2$ . This scenario has been dubbed the *quantized Hall insulator*. On the other hand, theoretical predictions show that a diverging  $R_H$  should be expected, i.e.,  $R_H \propto R_L^\alpha$  [22, 23]. This *Hall insulator* is to be expected at strong disorder or strong magnetic fields.

In fully quantum coherent transport measurements such as in mesoscopic devices at low temperature, the results clearly show the paramount influence of quantum interference and the measured quantities fluctuate strongly [24]. At magnetic field  $B = 0$ , the universal conductance fluctuations provide the most famous example [25]. For the QH situation, similarly reproducible and pronounced fluctuations have been observed previously [26, 27, 28, 29, 30, 31, 32, 33, 34], although no complete understanding of their behavior has yet emerged. Thus for quantum coherent QH samples, the average values  $R_L$  and  $R_H$  become meaningless unless

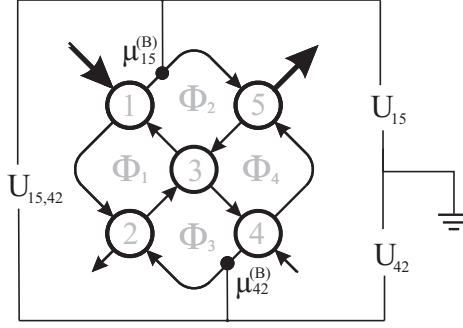


Fig. 1 – RG unit of 5 SP's (full circles) and equipotential lines (arrows) on a square lattice with Eq. (1) combining them into a super-SP.  $\Phi_1, \dots, \Phi_4$  are the phases acquired by an electron drifting along the contours. Arrows show the electron motion for one  $B$  direction and should be reversed for  $-B$ . The small solid dots indicate the position of the weakly-coupled voltage probes. The thin lines denote the different possibilities of measuring voltage drops in the present structure for both  $B$ -field directions.

their full distributions are being taken into account [35]. Consequently, different averaging procedures may then yield quite different estimates for  $R_L$  and  $R_H$ .

In the present manuscript, we revisit the Hall insulating regime by using a real-space renormalization group approach to the Chalker-Coddington network model. This method has recently been used successfully to study the energy-level statistics at the QH transition [36] as well as the influence of long-range correlations in the disorder potential close to the transition [37]. We will show that within the same model, we can find quantized *and* diverging behavior for  $R_H$  by simply changing the procedure used for averaging the distribution functions for  $R_L$  and  $R_H$ .

*Model and RG approach to the QH situation.* – The CC model is based on the microscopic picture of electron motion in a strong magnetic field and a smooth disorder potential [38] when only the semiclassical trajectories of the guiding center of the cyclotron orbit are important. Assigning these trajectories to *links* and considering saddle points (SP's) at which different trajectories come closer than the Larmor radius as *nodes* a chiral network can be constructed.

We now apply a real-space RG approach [28,39] to the CC network [30,40,41,42,36,23,37]. The RG unit we use is extracted from a CC network on a regular 2D square lattice as shown in Fig. 1. A super-SP consists of five original SP's by analogy to the RG unit employed for the 2D bond percolation problem [43,44,45]. Each SP can be described by two matrix equations relating the wave-function amplitudes in incoming and outgoing channels. Between the SP's an electron travels along equipotential lines, and accumulates a certain Aharonov-Bohm phase  $\Phi$ . Different phases are uncorrelated, which reflects the randomness of the original potential landscape. This results in a system of ten linear equations, the solution of which yields the expression for the transmission coefficient of the super-SP (Ref. [28]):

$$t' = \left| \frac{t_1 t_5 (r_2 r_3 r_4 e^{i\Phi_2} - 1) + t_2 t_4 e^{i(\Phi_3 + \Phi_4)} (r_1 r_3 r_5 e^{-i\Phi_1} - 1) + t_3 (t_2 t_5 e^{i\Phi_3} + t_1 t_4 e^{i\Phi_4})}{(r_3 - r_2 r_4 e^{i\Phi_2}) (r_3 - r_1 r_5 e^{i\Phi_1}) + (t_3 - t_4 t_5 e^{i\Phi_4}) (t_3 - t_1 t_2 e^{i\Phi_3})} \right|. \quad (1)$$

Here  $t_i$  and  $r_i = (1 - t_i^2)^{1/2}$  are, respectively, the transmission and reflection coefficients of the constituting SP's,  $\Phi_j$  are the phases accumulated along the closed loops (see Fig. 1).

Equation (1) is the RG transformation, which allows one to generate (after averaging over  $\Phi_j$ ) the distribution  $P(t')$  of the transmission coefficients of super-SP's using the distribution  $P(t)$  of the transmission coefficients of the original SP's. Since the transmission coefficients of the original SP's depend on the electron energy  $\varepsilon$ , the fact that delocalization occurs at  $\varepsilon = 0$  implies that a certain distribution,  $P_c(t)$  — with  $P_c(t^2)$  being symmetric with respect to  $t^2 = \frac{1}{2}$  — is a fixed point (FP) of the RG transformation (1). The distribution  $P_c(G)$  of the dimensionless two-point conductance  $G$  can be obtained from the relation  $G = t^2$ , so that  $P_c(G) \equiv P_c(t)/2t$ . We remark that the classical percolation limit [43, 44, 45] is obtained when the classical values  $t \in \{0, 1\}$  are used in the RG.

In a previous study, the problem of the QH insulator had been considered theoretically by an analytical RG approach, necessitating a further simplified 4SP RG structure [23]. As shown in Ref. [46], this 4SP is less reliable when applied to the QH transition regime. We emphasize that the 4SP structure is incorporated into our present 5SP when SP "3" in Fig. 1 is tuned to perfectly transmitting or reflecting.

Let us now make contact with the resistances. The *dimensionless* longitudinal resistance  $R_L$  can be computed from  $G$  via

$$R_L = \frac{|r|^2}{|t|^2} = \frac{1 - |t|^2}{|t|^2} = \frac{1}{G} - 1 \equiv R_{2t} - 1 \quad (2)$$

where  $R_{2t}$  is the dimensionless 2-terminal resistance. In order to study the Hall resistance for the four-terminal CC model, we follow Refs. [22, 23] and study the difference in (normalized) chemical potentials between source  $\mu_{15}$  and drain  $\mu_{42}$  at the positions indicated in Fig. 1. In order to remove any cross-current amplitudes, the voltage is computed, analogously to the experimental situation, by subtracting opposite magnetic field directions. The Hall voltage is then defined as

$$U_H = \frac{1}{2} \{ [\mu_{15}(B) - \mu_{42}(B)] - [\mu_{15}(-B) - \mu_{42}(-B)] \} \quad (3)$$

Consequently, the *dimensionless* Hall resistance is given by

$$R_H = \frac{U_H}{G} \quad (4)$$

*Numerical RG procedure.* — In order to find the FP distributions  $P_c(R_L)$  and  $P_c(R_H)$  at the QH transition, we start from an appropriate initial distribution of transmission coefficients,  $P_0(t)$ . In [36], we had shown that this procedure results in a broad FP distribution  $P_c(G)$  which is peaked at  $G \gtrsim 0$  and  $G \lesssim 1$ . Any RG flow away from this instable FP towards the insulating regimes will result in a further increase of one of these peaks. Therefore, in order to reliably model the insulating regime, an accurate procedure for reproducing these peaks is needed. In [36], we had also shown that the distribution  $Q(z)$  of dimensionless SP heights is related to  $P(G)$  via  $Q(z) = P(G)(dG/dz) = \frac{1}{4} \cosh^{-2}(z/2) P[(e^z + 1)^{-1}]$  and  $t = (e^z + 1)^{-1/2}$ . Thus the peaks in  $P(G)$  transform into long but quickly decaying tails in  $Q(z)$  and it is numerically much better to perform the RG for SP heights  $z$  when the physics away from the FP is studied.

We discretize the distribution  $Q(z)$  in at least 6000 bins such that the bin width is typically 0.01. Since  $z \in ]-\infty, \infty[$ , we have to include lower and upper cut-off SP heights such that  $z \in [z_{\text{low}}, z_{\text{up}}]$ . We use  $z_{\text{low}} = -20$ ,  $z_{\text{up}} = 40$  for perturbations towards positive  $z$  and vice versa for negative perturbations. This corresponds to transmission amplitudes  $t(z_{\text{low}}) \approx 10^{-5}$ ,  $t(z_{\text{up}}) \approx 1 - 10^{-9}$  for positive perturbations and vice versa for negative perturbations. From

$Q_0(z)$ , we obtain  $z_i$ ,  $i = 1, \dots, 5$ , compute the associated  $t_i$  and substitute them into the RG transformation (1). The phases  $\Phi_j$ ,  $j = 1, \dots, 4$  are chosen randomly from the interval  $\Phi_j \in [0, 2\pi]$ . In this way we calculate at least  $10^8$  super-transmission coefficients  $t'$  and associated  $z'$ . At the next step we repeat the procedure using  $Q_1$  as an initial distribution. We assume that the iteration process has converged when the mean square deviation  $\int dt [Q_n(t) - Q_{n-1}(t)]^2$  of the distribution  $Q_n$  and its predecessor  $Q_{n-1}$  deviate by less than  $10^{-4}$ . We check that the values of  $z_{\text{low,up}}$  do not influence our results and that all the previous results at the QH transition as in Refs. [36, 37] are reproduced. The full width at half maximum of the FP distribution  $Q_c(z)$  is about 5 [36].

*FP distributions.* – In Figs. 2 and 3, we show the FP distributions for  $R_L$  and  $R_H$ , respectively. As seen previously [22], both distributions are manifestly non-Gaussian with rather long tails. Indeed,  $P(R_L)$  can be fitted by a log-normal distribution as indicated in Fig. 2 [22]. The FP distribution  $P(R_H)$  exhibits a pronounced peak at  $R_H = 1$  ( $h/e^2$  in SI units) and a small shoulder around  $R_H = 0$ . The small weight for negative Hall resistivities shows that in the coherent RG structure chosen, the large fluctuations in  $P(t)$  can result in an apparent reversal of the Hall voltage. We note that these features persist even when taking instead of the 5SP RG structure the 4SP structure of Ref. [23].

*The plateau-insulator transition.* – In order to model the transition into the insulating regime, we now shift the initial distribution  $Q_0(z) \rightarrow Q_0(z - z_0)$  by a small  $z_0$ . For  $z_0 < 0$  and  $z_0 > 0$ , the RG flow will then drive the distributions into the insulating,  $G \rightarrow 0$ , and plateau,  $G \rightarrow 1$ , regimes, respectively. In Figs. 2 and 3, we show the resulting distributions after many RG steps. For  $P(R_L)$ , we see in Fig. 2 that the flow towards  $G \rightarrow 1$  results in a decrease of large  $R_L$  events, whereas conversely, the regime  $G \rightarrow 0$  leads to an increase in large  $R_L$  values and a decrease of the maximum value in  $P(R_L)$ . For  $P(R_H)$ , Fig. 3 shows that the plateau regime  $G \rightarrow 1$  gives a highly singular peak at the dimensionless quantized Hall value

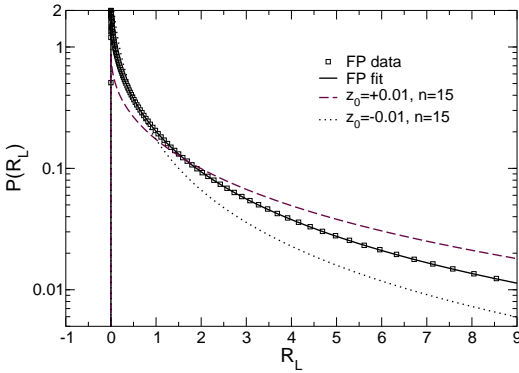


Fig. 2

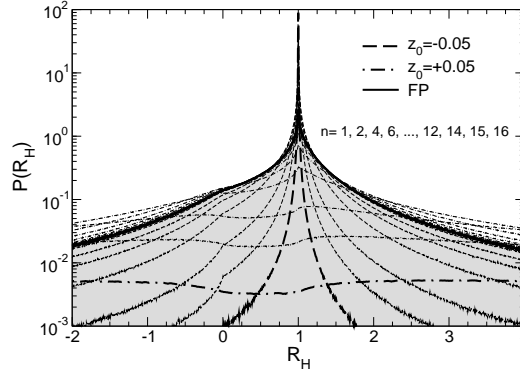


Fig. 3

Fig. 2 – Distribution of the longitudinal resistivity  $R_L$ . The  $\square$  symbols indicate the FP distribution, the solid line is a fit to a log-normal distribution and the dotted and dashed lines show the distribution after  $n = 15$  RG iterations into the conductance regimes  $G(z_0 < 0) \rightarrow 1$  and  $G(z_0 > 0) \rightarrow 0$ . Only every 5th data point is shown for  $P(R_L)$

Fig. 3 – Distribution of the Hall resistivity  $R_H$ . The FP distribution has been shaded to zero. For the  $G(z_0 < 0) \rightarrow 1$  and  $G(z_0 > 0) \rightarrow 0$  regimes, we have indicated the distributions after  $n = 16$  RG iterations by bold dashed and dashed-dotted lines.

1, corresponding to a perfect Hall plateau. On the other hand, the insulating regime  $G \rightarrow 0$  shows an increase of weight in the tails of  $P(R_H)$  and the eventual obliteration of any central peak.

In order to extract an averaged  $R_L$  and  $R_H$  from these non-standard distributions, we should now select an appropriate mean  $\langle \cdot \rangle$  that characterizes and captures the essential physics and allows comparison with the experimental data. The precise operational definition is also important as it corresponds to different possible experimental setups. Therefore, we consider several means: (i) arithmetic  $\langle R \rangle_{\text{ari}} = \sum_i R_i / N$ , (ii) geometric/typical  $\langle R \rangle_{\text{typ}} = \exp \sum_i \ln R_i / N$ , (iii) median (central value)  $\langle R \rangle_{\text{med}}$ , where  $N$  denotes the number of samples ( $\gtrsim 10^8$ ) in each case. The median and the typical mean (and their variances [23]) are less sensitive to extreme values than other means (such as, e.g. root-mean-square and harmonic mean) and this makes them a better measure for highly skewed and long-tailed distributions such as  $P(R_L)$  and  $P(R_H)$  in the insulating regime. In the plateau regimes, the distributions are less skewed, particularly for  $R_H$  and the difference in the means becomes less important.

We are left with determining in which operational order to apply the averaging procedure. For  $R_L$ , as measured via Ohm's law (2) as a ratio, it is obvious that the appropriate average should be  $\bar{R}_L = \frac{1}{\langle G \rangle} - 1$  (and not  $\langle \frac{1}{G} \rangle - 1$ ). For  $R_H$ , the situation is less straightforward due to the definition of  $U_H$  in (3). A simple average is  $\langle U_H \rangle$ , i.e. using the appropriate  $P(R_H)$ . Similar to the experimental procedure, we can also estimate  $\bar{U}_H$  via  $\langle \mu_{15} - \mu_{42} \rangle$  for each  $B$  field direction separately. In Ref. [23], it has been suggested that a more appropriate average  $\bar{U}_H$  can be constructed from  $\langle \mu_{15} \rangle - \langle \mu_{42} \rangle$ . This later procedure corresponds to measuring the voltage drop between positions  $\mu_{15}$  and  $\mu_{42}$  in Fig. 1 by separately measuring the individual voltages with respect to ground and then recombining them.

In Fig. 4 we show the resulting dependence  $R_H(R_L)$  when these averaging definitions are being used. This figure is our main result. As shown, for  $R_L \rightarrow \infty$ , we get a divergent  $R_H$  when using the median and typical means as suggested by Refs. [22, 23] to compute both  $R_L$  and  $R_H$ . This divergence can be captured by a power-law  $R_H \propto R_L^\kappa$  with  $\kappa \approx 0.26$ . On the other hand, a nearly constant behavior of  $R_H$  in the insulating regime can be seen when instead we use arithmetic means, neglecting numerically instable fluctuations for extreme  $P_H$  values by constraining  $P(R_H) \gtrsim 10^{-3}$  or  $R_H \in [1 - 99, 1 + 99]$  symmetric around 1. Last, when interchanging some of these means, the value of  $\kappa$  can be made to vary substantially as shown in Fig. 4. Such a situation appears relevant in any experimental setup where  $10^8$  different samples cannot be easily measured and the full distribution functions cannot be constructed in similar detail.

Fig. 4 contains large resistance values. Reducing the information to the experimentally more relevant resistance regimes of a few times  $h/e^2$ , we see in Fig. 5 a plot of  $R_L$  and  $R_H$  closer to the transition. We emphasize that on this scale, the value of  $\langle R_H \rangle_{\text{ari}}$  deviates only slightly from its quantized value 1 at the transition and  $R_L + R_H \approx R_{2t}$  [33]. Therefore, the arithmetic data appears to support the notion of the quantized Hall insulator, but the value of  $\langle R_H \rangle_{\text{ari}}$  is of course subject to the chosen cut-off. The typical means are also not far from 1 and the precise nature of the power-law divergence has not yet established itself. We also note that the relation  $R_L(z_0) = 1/R_L(-z_0)$  is obeyed by all means [47]. This is a consequence of the reflection symmetry of  $P(G)$  [36].

The results for  $R_L$  and  $R_H$  in the localized regime can be very well described by an exponential scaling function with finite-size correction [22]  $R_{L,H}(2^n, z) \propto 2^{\gamma n} \exp \left[ 2^n \xi_{L,H}^{-1}(z) \right]$ . Plotting  $\xi_{L,H}$  as a function of small perturbation  $z_0$ , we find  $\xi_{L,H}(z_0) \propto z_0^{-\nu_{L,H}}$  with  $\nu_{L,H} \approx 2.35$ . Thus we recover the universal divergence of the localization length  $\xi$  even when using the RG in the insulating regime [22]. An equally reliable estimate of the irrelevant exponent

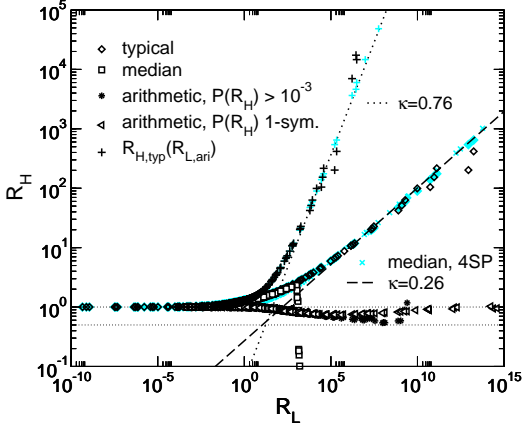


Fig. 4

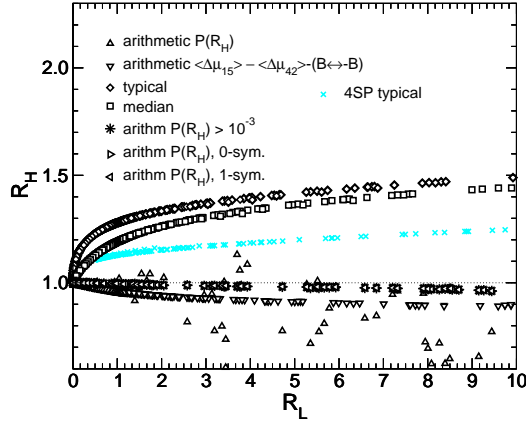


Fig. 5

Fig. 4 – Dependence of averaged  $R_H$  on averaged  $R_L$  for 5 and 4 SP RG structures and various means as indicated. When using for both  $R_L$  and  $R_H$  the *typical* means or the median, the divergence  $R_H \propto R_L^\kappa$  can be fitted with  $\kappa \approx 0.26$ . Arithmetic means ( $\ast$ ,  $\nabla$ , see text) remain close to 1. A non-consistent interchange of various limits can give rise to yet different divergencies as indicated by the  $+$  symbols. The horizontal dotted lines indicate  $R_H = 1$  and  $1/2$ . Grey symbols denote equivalent data obtained from passing current through the lower parts of Fig. 1. This is numerically more stable, but corresponds to different samples for each  $B$ -field direction.

Fig. 5 – Plot of similar data as in Fig. 4 but on a linear scale and for experimentally accessible resistance values. Here the almost quantized behavior for the arithmetic means becomes even more pronounced. Fluctuations in the arithmetic mean of the distribution  $P(R_H)$  ( $\Delta$ ) are reduced when instead considering  $\langle \Delta \mu_{15} \rangle_{\text{ari}} - \langle \Delta \mu_{42} \rangle_{\text{ari}} - (B \leftrightarrow -B)$  ( $\nabla$ ) or again neglecting numerically instable, large  $R_H$  (small  $T \lesssim 10^{-13}$ ) events ( $\ast, \triangleright, \triangleleft$ ). The horizontal dotted line indicates  $R_H = 1$ . Grey symbols as in Fig. 4.

$\gamma$  appears not possible for our data.

As usual, the 4-terminal resistances can be converted into the respective conductances via  $\sigma_{L,H} = R_{L,H} / (R_L^2 + R_H^2)$ . For these conductances, one expects the semi-circle law  $\sigma_L^2 + (\sigma_H - 1/2)^2 = (1/2)^2$  to hold [48]. In Fig. 7, we show that the arithmetic means, giving rise to an apparently quantized  $R_H$  in Fig. 5, capture the overall shape and symmetry properties, but the other averages show pronounced deviations.

Stimulating discussions with B. Huckestein, B. Muzykantskii, M. E. Raikh, and U. Zülicke are gratefully acknowledged. This research is supported by the DFG within the Schwerpunktprogramm “Quanten-Hall-Systeme” and the SFB 393.

## REFERENCES

- [1] H. P. Wei, D. C. Tsui, and A. M. M. Pruisken, Phys. Rev. B **33**, 1488 (1985).
- [2] H. P. Wei, D. C. Tsui, M. A. Paalanen, and A. M. M. Pruisken, Phys. Rev. Lett. **61**, 1294 (1988).
- [3] S. Koch, R. J. Haug, K. v. Klitzing, and K. Ploog, Phys. Rev. B **43**, 6828 (1991).
- [4] S. Koch, R. J. Haug, K. v. Klitzing, and K. Ploog, Phys. Rev. Lett. **67**, 883 (1991).
- [5] S. Koch, R. J. Haug, K. v. Klitzing, and K. Ploog, Phys. Rev. B **46**, 1596 (1992).
- [6] H. P. Wei, S. Y. Lin, D. C. Tsui, and A. M. M. Pruisken, Phys. Rev. B **45**, 3926 (1992).

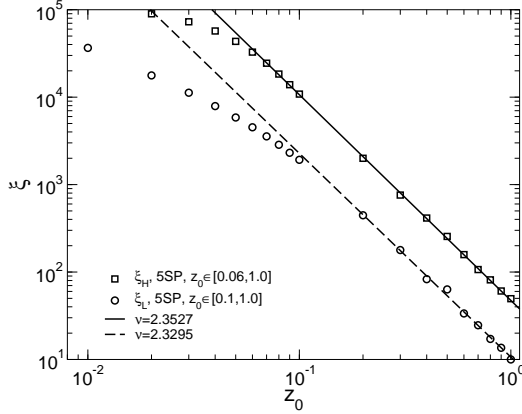


Fig. 6

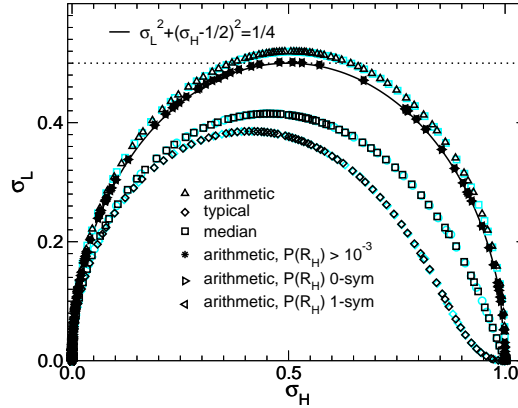


Fig. 7

Fig. 6 – Dependence of the localization lengths  $\xi_L$  and  $\xi_H$  on the initial shift  $z_0$  using the ansatz (8) of [22]. We obtain a reasonable estimate of the critical exponent  $\nu$ .

Fig. 7 – The semi circle law for different means as in Fig. 5. The stabilized arithmetic means ( $*$ ,  $\triangleright$ ,  $\triangleleft$ ) show perfect semi-circle (solid line) behaviour. The thin dotted line denotes  $\sigma_L = 1/2$ . Grey symbols as in Fig. 4.

- [7] S. W. Hwang, H. P. Wei, L. W. Engel, D. C. Tsui, and A. M. M. Pruisken, Phys. Rev. B **48**, 11416 (1993).
- [8] F. Kuchar, R. Meisels, K. Dybko, and B. Kramer, Europhys. Lett. **49**, 480 (2000).
- [9] F. Hohls, U. Zeitler, R. J. Haug, and K. Pierz, Physica B **298**, 88 (2001), ArXiv: cond-mat/0010417.
- [10] F. Hohls, U. Zeitler, and R. J. Haug, Phys. Rev. Lett. **86**, 5124 (2001), ArXiv: cond-mat/0011009.
- [11] R. T. F. van Schaijk, A. de Visser, S. M. Olsthoorn, H. P. Wei, and A. M. M. Pruisken, Phys. Rev. Lett. **84**, 1567 (2000).
- [12] V. Goldman, J. Wang, B. Su, and M. Shayegan, Phys. Rev. Lett. **70**, 647 (1993).
- [13] W. Pan, D. Shahar, D. C. Tsui, H. P. Wei, and M. Razeghi, Phys. Rev. B **55**, 15431 (1997).
- [14] D. Shahar, D. C. Tsui, M. Shayegan, J. E. Cunningham, E. Shimshoni, and S. L. Sondhi, Solid State Commun. **102**, 817 (1997).
- [15] S. Murphy, J. Hicks, W. Liu, S. Chung, K. Goldammer, and S. M.B., Physica E **6**, 293 (2000).
- [16] D. Shahar, D. C. Tsui, M. Shayegan, R. N. Bhatt, and J. E. Cunningham, Phys. Rev. Lett. **74**, 4511 (1995).
- [17] M. Hilke, D. Shahar, S. Song, D. Tsui, Y. Xie, and D. Monroe, Nature **395**, 675 (1998).
- [18] D. Shahar, D. Tsui, M. Shayegan, E. Shimshoni, and S. Sondhi, Science **274**, 1 (1996).
- [19] R. Hughes, J. Nicholls, J. Frost, E. Linfield, M. Pepper, C. Ford, D. Ritchie, G. Jones, E. Kogan, and M. Kaveh, J. Phys.: Condens. Matter **6**, 4763 (1994).
- [20] D. Shahar, D. C. Tsui, M. Shayegan, E. Shimshoni, and S. L. Sondhi, Phys. Rev. Lett. **79**, 479 (1997).
- [21] D. de Lang, L. Ponomarenko, A. de Visser, C. Possanzini, S. Olsthoorn, and A. Pruisken, Physica E **12**, 666 (2002).
- [22] L. P. Pryadko and A. Auerbach, Phys. Rev. Lett. **82**, 1253 (1999).
- [23] U. Zülicke and E. Shimshoni, Phys. Rev. B **63**, 241301 (2001), ArXiv: cond-mat/0101443.
- [24] J. K. Jain and S. A. Kivelson, Phys. Rev. Lett. **60**, 1542 (1988).
- [25] P. A. Lee, A. D. Stone, and H. Fukuyama, Phys. Rev. **35**, 1039 (1987).
- [26] D. H. Cobden and E. Kogan, Phys. Rev. B **54**, R17316 (1996).

- [27] D. H. Cobden, C. H. W. Barnes, and C. J. B. Ford, Phys. Rev. Lett. **82**, 4695 (1999).
- [28] A. G. Galstyan and M. E. Raikh, Phys. Rev. B **56**, 1422 (1997).
- [29] Z. Wang, B. Jovanovic, and D.-H. Lee, Phys. Rev. Lett. **77**, 4426 (1996).
- [30] A. Weymer and M. Janssen, Ann. Phys. (Leipzig) **7**, 159 (1998), ArXiv: cond-mat/9805063.
- [31] S. Cho and M. P. A. Fisher, Phys. Rev. B **55**, 1637 (1997).
- [32] B. Jovanovic and Z. Wang, Phys. Rev. Lett. **81**, 2767 (1998).
- [33] E. Peled, D. Shahar, Y. Chen, E. Diez, D. L. Sivco, and A. Y. Cho, (2003), cond-mat/0307423.
- [34] E. Peled, D. Shahar, Y. Chen, D. L. Sivco, and A. Y. Cho, Phys. Rev. Lett. **90**, 246802 (2003).
- [35] O. Entin-Wohlman, A. Aronov, Y. Levinson, and Y. Imry, Phys. Rev. Lett. **75**, 4094 (1995).
- [36] P. Cain, R. A. Römer, M. Schreiber, and M. E. Raikh, Phys. Rev. B **64**, 235326 (2001), ArXiv: cond-mat/0104045.
- [37] P. Cain, R. A. Römer, and M. E. Raikh, Phys. Rev. B **67**, 075307 (2003), ArXiv: cond-mat/0209356.
- [38] J. T. Chalker and P. D. Coddington, J. Phys.: Condens. Matter **21**, 2665 (1988).
- [39] D. P. Arovas, M. Janssen, and B. Shapiro, Phys. Rev. B **56**, 4751 (1997), ArXiv: cond-mat/9702146.
- [40] M. Janssen, R. Merkt, and A. Weymer, Ann. Phys. (Leipzig) **7**, 353 (1998).
- [41] M. Janssen, R. Merkt, J. Meyer, and A. Weymer, Physica **256–258**, 65 (1998).
- [42] J. Sinova, V. Meden, and S. M. Girvin, Phys. Rev. B **62**, 2008 (2000), ArXiv: cond-mat/0002202.
- [43] D. Stauffer and A. Aharony, *Introduction to Percolation Theory* (Taylor and Francis, London, 1992).
- [44] P. J. Reynolds, W. Klein, and H. E. Stanley, J. Phys. C **10**, L167 (1977).
- [45] J. Bernasconi, Phys. Rev. B **18**, 2185 (1978).
- [46] P. Cain, R. A. Römer, and M. E. Raikh, J. Phys. Soc. Japan (2003).
- [47] D. Shahar, M. Hilke, C. C. Li, D. C. Tsui, S. L. Sondhi, and M. Razeghi, Solid State Commun. **107**, 19 (1998), ArXiv: cond-mat/9706045.
- [48] I. Ruzin and S. Feng, Phys. Rev. Lett. **74**, 154 (1995).